Electronic energy spectrum of two-dimensional solids and a chain of C atoms from a quantum network model

Claudio Amovilli*

*Dipartimento di Chimica e Chimica Industriale, Università di Pisa, Via Risorgimento 35,
I-56126 Pisa, Italy*
E-mail: amovilli@dcci.unipi.it

Frederik E. Leys and Norman H. March[1]

Department of Physics, University of Antwerp, Groenenborgerlaan 171,

B-2020 Antwerpen, Belgium

The aim of this study is to explain how a quantum network can be used as simple model to calculate complex band structures. The paper contains an introduction, a mathematical exposure of the method, and applications to graphene, boron nitride, and polyacetylene chains. Using a quantum network is a simple, intuitive, and, yet, rather accurate way to obtain a band structure for a complex material. One focus here is to invoke physical and chemical intuition to construct the effective one-body potential along the wires of a quantum network.

KEY WORDS: quantum network model, electronic energy bands, density of states, two-dimensional lattices, connectivity

AMS subject classification: 81Q05, 82D26, 65C40

1. Background

The quantum network model [1–4] reduces the multicentre problems posed by periodic solids such as graphite and boron nitride, to be treated in some detail below, to what is essentially an application of Kirchoff's laws in an electrical circuit. By way of illustration let us start with three-dimensional graphite depicted as to its crystal structure in figure 1. It consists of rather weakly interacting hexagonal planes of C atoms. The weak coupling between planes is clear from the fact that while the nearest C–C spacing in one plane (known as graphene) is

---

*Corresponding author.

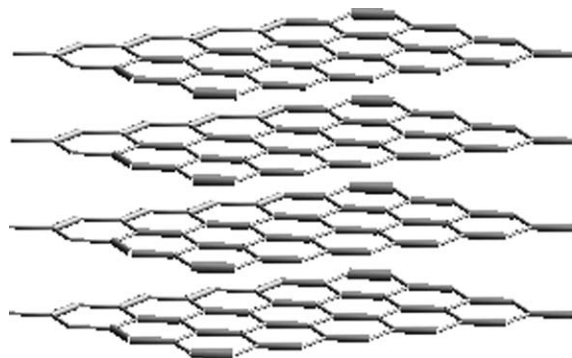[1]Oxford University, Oxford, England

Figure 1.   Crystal structure of graphite.

1.43 Å, the interlayer separation is 3.5 Å. Thus, it is already a valuable approximation to the electronic structure of three-dimensional graphite to treat a single layer, namely graphene. This is shown in figure 2(a), where "wires" connect each C atom to its nearest-neighbours. One can view figure 2(a), very helpfully, as an electrical circuit in which currents flow in a manner governed by Kirchoff's laws. Free electrons on zig–zag wires and various ring structures have been used by a number of authors [1,2,5–7].

   In the simplest version of such a model, worked out by Coulson [2], current conservation constituted a "boundary condition" at every junction, whereas he assumed that in their motion along the wires of the "graphene" network the valence (π) electrons were free: i.e. electrons moved in zero potential energy $V = 0$. One impressive, and indisputable, finding of Coulson was that the π-electron energy bands of graphene touched at the Fermi energy E_f, with zero density of states there, i.e. $N(E_f) = 0$ (see figure 6 below, with however a potential $V \neq 0$ along the wires). Thus, a single graphene layer, in solid-state parlance, was correctly predicted by the Kirchoff network laws as having semimetallic character.

   In the present study, we take advantage of progress in the quantum network model (QNM) especially notable work being that of Montroll [4], to give a mathematically rather complete version of the theory as applied to periodic systems like graphite and boron nitride crystals.

   The outline of the paper is then as follows. In Section 2 the QNM is applied to a graphene layer, which has been set out in a 'self-contained" form. Section 3 generalises the C layer treatment of the previous section to deal with a BN layer (figure 2(b)) having the same hexagonal structure, and again the presentation of this example is complete in itself. The polyacetylene infinite chain with alternating single and double bonds (figure 2(d)) is the subject of Section 4. These examples then prompt a more formal section, getting out fully the mathematics underlying the QNM. A summary, with some suggestions for possible future studies, constitutes the final Section 6.
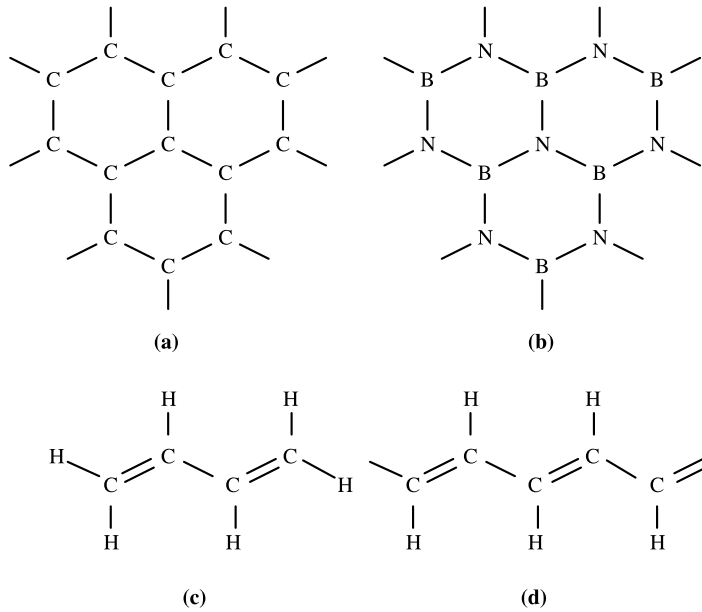
Figure 2. Structures of systems considered in this work. (a) Portion of infinite graphene layer. (b) Similar to (a) but for boron nitride. (c) Butadiene molecule, which is used to fix potential energy along wires in the QNM of carbon compounds. (d) *trans*-Polyacetylene.

2. Application of QNM to a single hexagonal plane of C atoms: Graphene valence electrons

We shall first set out a treatment of the graphene layer of figure 2(a), as a Kirchoff electrical network, but transcending previous treatments by constructing of an effective one-body potential in which electrons move on the wires.

Along the lines joining the near-neighbour C atoms, the wave functions satisfy one-dimensional Schrödinger equations, which are formally set out in Section 5. Knowing the wave functions along the wires by solution of these Schrödinger equations, one parallels the Kirchoff electrical network by imposing that at every junction of the two-dimensional graphene layer, probability flow (corresponding to electrical current) must be conserved. Additionally, however, in a periodic lattice, in this example two-dimensional, Bloch's theorem must be satisfied: i.e. the wave function on one wire is a product of a free-particle term times a periodic function with the period of the lattice. We note next, again making contact with Kirchoff's law, that current $\vec{j}$ corresponding to such a complex Bloch wave function ϕ is given by

$$\vec{j} = \mathrm{i}\left(\phi^* \vec{\nabla}\phi - \phi\vec{\nabla}\phi^*\right).$$ (1)

Proceeding to solve the Schrödinger equation between junctions, one can write a solution

$$\phi_{lm}(x) = F_{lm}(x)\phi_{lm}(0) + G_{lm}(x)\phi'_{lm}(0), \tag{2}$$

which represents the general solution of a second-order Schrödinger differential equation along the wire joining the junctions l and m in terms of $F_{lm}(x)$ and $G_{lm}(x)$, namely the solutions with initial conditions $F_{lm}(0) = 1$, $F'_{lm}(0) = 0$ and $G_{lm}(0) = 0$, $G'_{lm}(0) = 1$.

Following Kirchoff's law (see Section 5 for full details) we are led to the QNM equations at the nodes of a graphene lattice unit cell.

The unit cell in graphene contains two carbon atoms, labelled a and b in figure 3, and the lattice is generated by two vectors $\vec{u}_1$ and $\vec{u}_2$. The QNM equations at the nodes of a unit cell become

$$3F_{CC}\Phi_a = \sum_{b'(a)} \Phi_{b'},$$

$$3F_{CC}\Phi_b = \sum_{a'(b)} \Phi_{a'}, \tag{3}$$

where the sums are restricted to the nearest-neighbours and the Φ_a and Φ_b are related to ϕ_{lm} in equation (2) by

$$\Phi_a = \phi_{ab}(x_a), \qquad \Phi_b = \phi_{ab}(x_b), \tag{4}$$

while $F_{CC} = F_{CC}(d_{CC})$, d_{CC} being the C–C bond length.
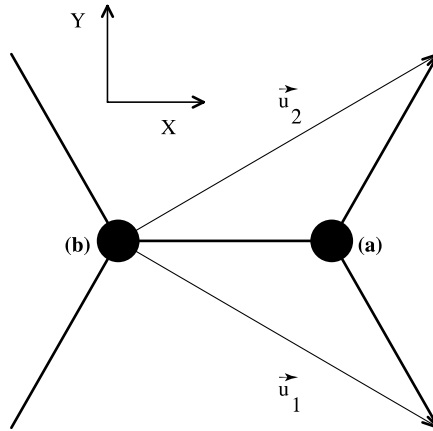

Figure 3.   Unit cell of a graphene layer. Also shown are lattice vectors $\vec{u}_1$ and $\vec{u}_2$.

Bloch's theorem applied to the two different C atom subsets leads to

$$3F_{CC}\Phi_a = \left(1 + e^{i\vec{k}\cdot\vec{u}_1} + e^{i\vec{k}\cdot\vec{u}_2}\right)\Phi_b,$$

$$3F_{CC}\Phi_b = \left(1 + e^{-i\vec{k}\cdot\vec{u}_1} + e^{-i\vec{k}\cdot\vec{u}_2}\right)\Phi_a. \tag{5}$$

2.1. Choice of wire potential V_{CC} along a near-neighbour bond in graphene

In energy band theory one is interested in the energy E as a function of the wave vector **k**, which in a graphene layer in the (x, y) plane has components $\mathbf{k} = (k_x, k_y)$. This so-called dispersion relation $E(\mathbf{k})$ can be calculated numerically from the relation

$$9F_{CC}^2 = \left(1 + e^{i\vec{k}\cdot\vec{u}_1} + e^{i\vec{k}\cdot\vec{u}_2}\right)\left(1 + e^{-i\vec{k}\cdot\vec{u}_1} + e^{-i\vec{k}\cdot\vec{u}_2}\right) \tag{6}$$

obtained by multiplying together the two equations (6). We remark that F_{CC} is the value at one node of a function satisfying a one-dimensional Schrödinger equation for a given eigenvalue E and for given boundary conditions.

The simplest QNM puts the potential $V(x)$ in the Schrödinger equation equal to zero: leading to the so-called free electron network model. Energy wave number relations, with this assumption, can only reflect the geometry of the graphene layer. It is significant, for more qualitative energy-band structure, to construct a somewhat realistic potential $V(x)$. A simple analytic form of $V(x)$ can appeal to the chemistry of a small molecule. We remark that the wave function ϕ of equation (2) is the analogue of a molecular orbital defined over a graph, the electrical network, instead of the whole space. In the present model ϕ is calculated by direct integration of Schrödinger equation instead of resorting to the most widely used approach known as linear combination of atomic orbitals (LCAO) approximation (see, for example [8]).

The potential V_{CC} we have used to treat this example and later also the polyacetylene is modelled in the following way:

$$V_{CC}(\lambda) = -0.85 + \frac{d_{CC}}{1.34}\sin^2\left(\frac{\pi\lambda}{d_{CC}}\right), \tag{7}$$

where energies are in units of $E_h = e^2/a_0$ and lengths in Å. d_{CC} is the distance between neighbour C atoms, which for graphene is 1.43 Å. The potential V_{CC} varies around the value –0.85 because of the $\sin^2$ term in equation (7) and the highest value of V_{CC} leads to energy barrier the height of which has been taken proportional to the C–C bond length and fixed at 1 E_h for an isolated double bond as results from figure 12 (see also Section 5). The value $-0.85E_h$ at the

nodes has been found instead by imposing that $F_{CC} = 1$ at the energy of the highest occupied molecular orbital of ethylene ($\Phi_1 = \Phi_2$ for symmetry reasons in this particular molecule).

2.2. Calculation of energy wave number relations for graphene layer

The dispersion relation $E(\mathbf{k})$ has been evaluated for a particular path in the wave vector space, usually referred as $K \equiv (2\pi/3, 2\pi/3\sqrt{3}) \rightarrow \Gamma \equiv (0,0) \rightarrow M \equiv (2\pi/3, 0) \rightarrow K$. The position of the symmetry points Γ, M and K on the Brillouin zone is shown in figure 4. Figure 5 finally shows the computed $E(\mathbf{k})$. These $E(\mathbf{k})$ curves transcend those of Coulson [2] as in figure 2(a) the electrons were moving in a potential energy V along each wire in the Kirchoff electrical network.

From the dispersion relation $E(\mathbf{k})$ the density of electronic energy states $N(E)$, defined such that $N(E)\mathrm{d}E$ is the number of electronic energy levels lying in the range E to $E + \mathrm{d}E$, has been calculated and is shown in figure 6. The valence (π) bands are seen to touch at the Fermi level, this being determined by the fact that the lowest sub-band is completely filled when one has 1 π-electron per C atom as in the graphene layer under consideration. The fact that with $V = 0$, as in Coulson's original study [2], and with non-zero potential V along the wires as in the present results depicted in figure 6, the same "touching" of the π-bands at the Fermi level is found indicates clearly that this crucial property of the electronic band structure of a graphene layer is "potential insensitive", and determined essentially by topological considerations. Of course, this is not generally true for $E(\mathbf{k})$ in figure 5 and $N(E)$ in figure 6: different potential energy forms along the wires of the Kirchoff network lead to quantitatively different dispersion relations and densities of states.
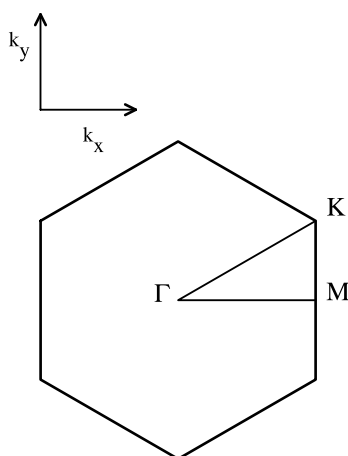

Figure 4. Brillouin zone for graphene layer showing the symmetry points Γ, M and K.
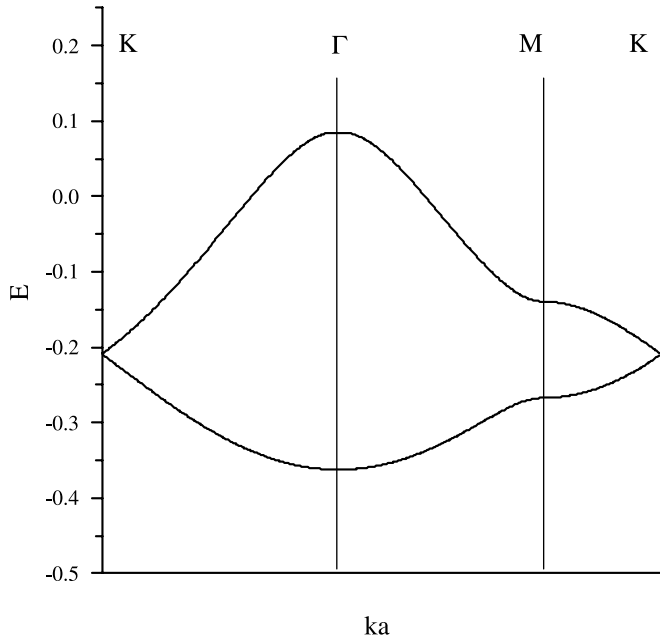
Figure 5. Dispersion relation $E(\mathbf{k})$ for π sub-bands of infinite graphene layer. Symmetry points labelled in figure 4 are marked on this present figure.

3. Introduction of electronegativity: the electronic energy gap between the π-sub-bands of a single hexagonal layer of boron nitride

Chemists use the concept of electronegativity to incorporate an ionic contribution to binding in molecules and solids. In probably its simplest form, the electronegativity of a neutral atom can be approximated by Mulliken's formula $(I + A)/2$, where I is the ionization potential and A the electron affinity. In passing from graphene to a BN single hexagonal layer, it is easy to verify that from the above formula there is a substantial electronegativity difference between B and N.

To incorporate this, it is now quite essential to invoke potentials which vary spatially along the wires of the appropriate Kirchoff network and, in contrast to graphene, the potential energy along a B–N wire has a difference in value at the B and N nodes. We shall see that, because of the electronegativity difference between B and N atoms, the π-bands, which touched at the Fermi level in graphene, are now pushed apart by a very substantial energy of some eV.

As for graphene, the planar lattice of boron nitride is characterised by a unit cell with B and N atoms replacing the C_a and C_b atoms with the same translational vectors $\vec{u}_1$ and $\vec{u}_2$. Thus, the system of QNM equations for this case is
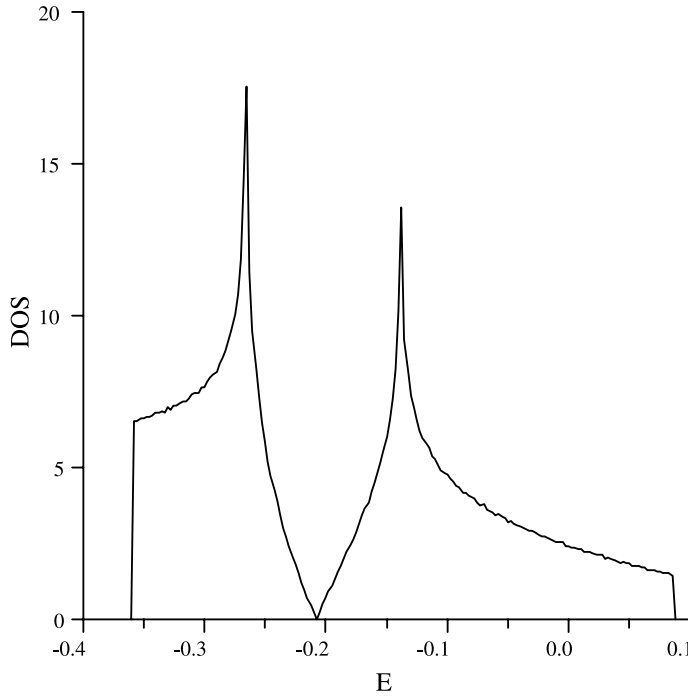
Figure 6. Density of π-electron states, $N(E)$ in the π sub-bands of an infinite graphene layer. Spikes shown occur at energies for which the group velocity $dE/d\vec{k}$ becomes zero. They represent the so-called Van Hove singularities [26].

$$3F_{BN}\Phi_B = \left(1 + e^{i\vec{k}\cdot\vec{u}_1} + e^{i\vec{k}\cdot\vec{u}_2}\right)\Phi_N,$$

$$3F_{NB}\Phi_N = \left(1 + e^{-i\vec{k}\cdot\vec{u}_1} + e^{-i\vec{k}\cdot\vec{u}_2}\right)\Phi_B,$$

(8)

where now $F_{BN} \neq F_{NB}$ due to the asymmetry of the potential V_{BN} along the wires connecting B and N atoms. The one-dimensional potential energy V_{BN} used to solve the Schrödinger equation along wires has been modelled in a parallel fashion to that already set out for the graphene layer:

$$V_{BN}(\lambda_{BN}) = -0.5 - 0.5\frac{\lambda_{BN}}{d_{BN}} + 0.75\sin^2\left(\frac{\pi\lambda_{BN}}{d_{BN}}\right),$$

(9)

in which, again, the energy is in E_h. d_{BN},the distance between neighbouring B and N atoms was set to $1.43\,\text{Å}$ as for graphene. In equation (9), the variable λ_{BN} is 0 at B junctions and d_{BN} at N junctions. With the above model function the potential energy difference between B and N junctions is thus $0.5E_h$ (13.6 eV). The potential energy is lower at the most electronegative atom, namely nitrogen. The numerical parameters in equation (9) have been deter-

mined by means of LCAO molecular orbital calculations performed on the borazole molecule, the property of which already reflect electronegativity difference between B and N. A plot of the potential V_{BN} along the BN wire is shown in figure 7 where it is compared also with the potential V_{CC} of equation (7).

Multiplying together the two equations (9), we have

$$9 F_{BN} F_{NB} = \left(1 + e^{i\vec{k}\cdot\vec{u}_1} + e^{i\vec{k}\cdot\vec{u}_2} \right) \left(1 + e^{-i\vec{k}\cdot\vec{u}_1} + e^{-i\vec{k}\cdot\vec{u}_2} \right), \qquad (10)$$

which can be solved numerically to get $E(\mathbf{k})$. Figures 8 and 9 show the resulting energies of π-bands, along the $K\Gamma MK$ path in reciprocal space, and the related density of states. Here, there is a gap between the two π-sub-bands of about 6.8 eV. In boron nitride the experimental value for the gap is 5.5 eV.
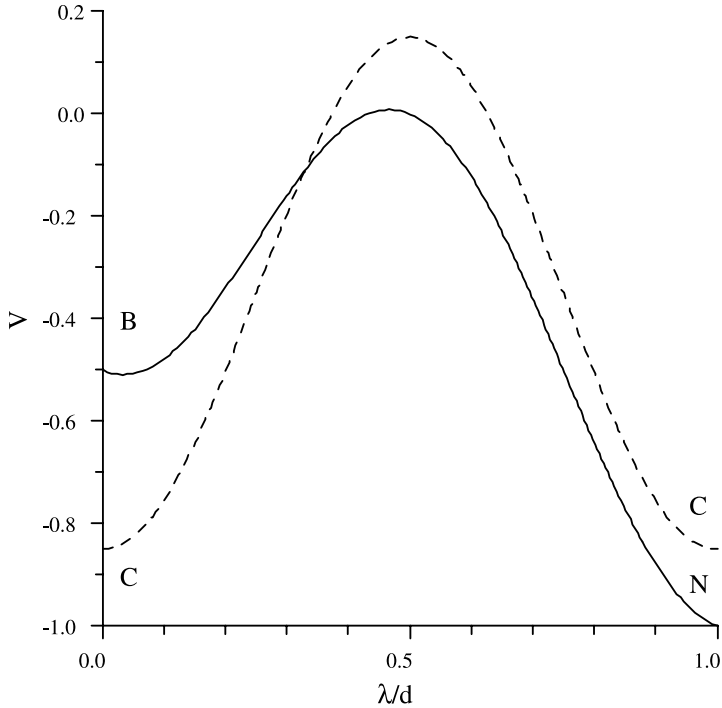

Figure 7. QNM effective potential for the B–N wires (solid line) and C–C wires (dashed line) used in this work to study the π-bands of graphene, boron nitride planar lattice and polyacetylene. The energies are in atomic units and λ/d varies between 0 and 1. d is the distance between the linked nodes.
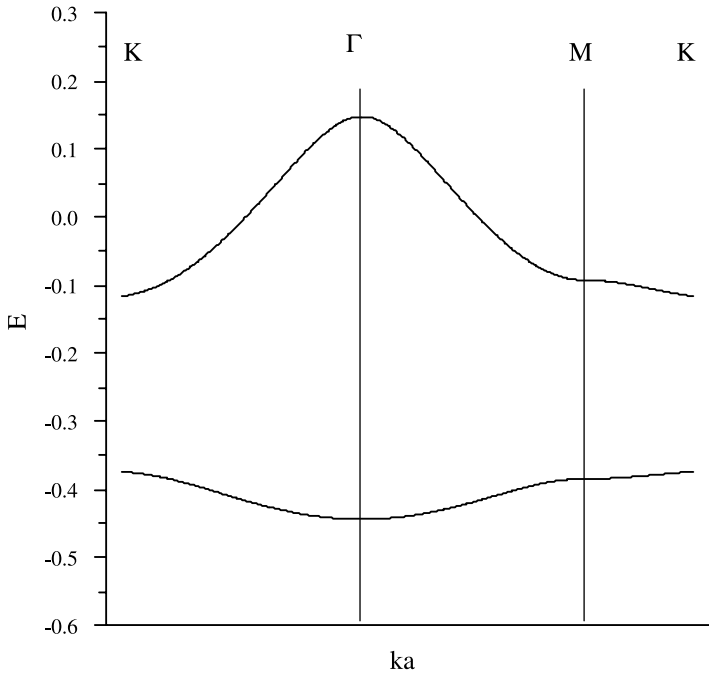
Figure 8. Similar to figure 5, but now for a single BN infinite layer. The large band gap opened between the π-electron sub-bands is a consequence of the electronegativity difference between B and N atoms.

## 4. Bond alternation and energy gap in polyacetylene

Polyacetylene represents an organic chain, and is known to exhibit bond length alternation, as shown in figure 2(d). Obviously without bond alternation there would be a free-electron one-dimensional spectrum and no energy gap.

The purpose of including this, apparently simpler, example at this stage is to exhibit directly the connection between the extent of bond alternation and the magnitude of the energy gap. Again the focus is on the π-electrons; one per C atom.

For a unit cell of *trans*-polyacetylene, the analogue of the QNM equations given for graphene in equation (4) is written below:

$$\left(\frac{F}{G} + \frac{f}{g}\right)\Phi_j = \frac{1}{G}\Phi_{j+1} + \frac{1}{g}\Phi_{j-1},$$

$$\left(\frac{F}{G} + \frac{f}{g}\right)\Phi_{j+1} = \frac{1}{G}\Phi_j + \frac{1}{g}\Phi_{j+2}.$$

$$(11)$$

Here bond length alternation in the chain is reflected in the appearance of the two pair of functions (F, G) and (f, g), where in full $(F, G) = (F_l, G_l)$ and
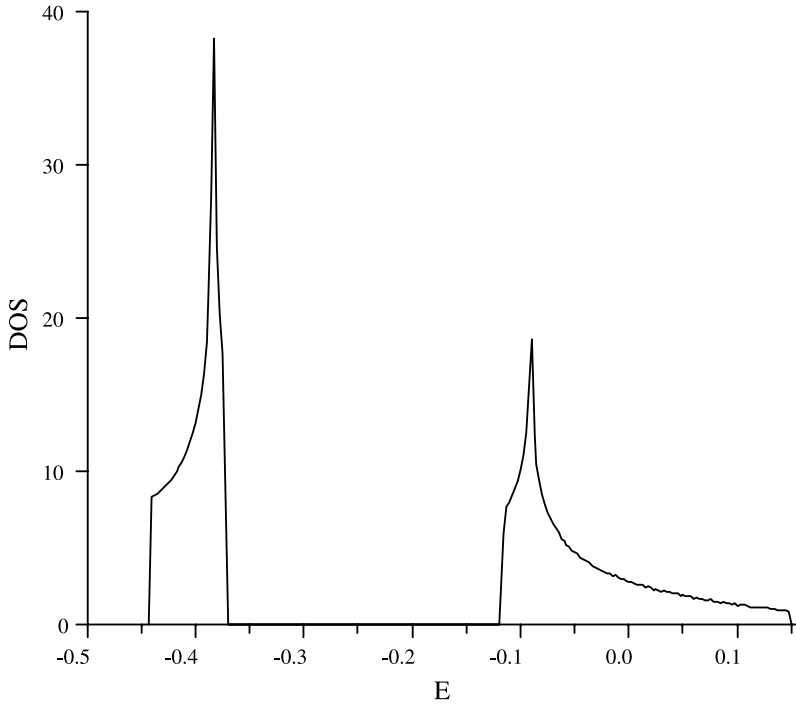
Figure 9. Density of π-electron states in BN layer.

$(f, g) = (f_s, g_s)$ where l and s refer to long and short C–C bonds, respectively (see Section 5 for full details). Following this, the imposition of Bloch's theorem along the chain, gives

$$\left(\frac{F}{G} + \frac{f}{g}\right) \Phi_j = \left(\frac{1}{G} + \frac{\mathrm{e}^{-ika}}{g}\right) \Phi_{j+1},$$

$$\left(\frac{F}{G} + \frac{f}{g}\right) \Phi_{j+1} = \left(\frac{1}{G} + \frac{\mathrm{e}^{ika}}{g}\right) \Phi_j,$$

$$(12)$$

where a denotes the sum of the short and long C–C bond lengths. As before, we form the product of equations (12) and (13) above to find

$$\left(\frac{F}{G} + \frac{f}{g}\right)^2 = \left(\frac{1}{G} + \frac{e^{-ika}}{g}\right)\left(\frac{1}{G} + \frac{e^{ika}}{g}\right). \qquad (13)$$

This equation has the structure $H(E, k) = 0$, which, by solution yields the one-dimensional dispersion relation of the π-electrons in the infinite polyacetylene chain.

The key information needed to plot numerically this $E(k)$ relation is the potential energy $V(\lambda)$ along now both long and short bonds. We assume the

transferability of the C–C potential used for graphene, and modelled by equation (7), provided along the two types of bond the appropriate bond length d_{CC} is inserted.

Figure 10 refers to the simplest case when there is no bond alternation and d_{CC} = 1.43 Å. Then there is no energy gap between the π sub-bands. Figure 11 now introduces bond alternation, characterised by the well known values 1.35 Å for the double bond and 1.53 Å for the single bond. The band gap is then 1.6 eV whereas Greenham and Friend [9] quote 1.5 eV. This agreement is remarkable and indeed better than could be expected from such a simple model.

Having established a basic feature – a band gap – depending on bond alternation, we will conclude this section by pointing out the potential of organic conductors for device physics. In particular, attention will be focussed on why polyacetylene has become a material of interest in this content. For the reader interested in an extended discussion the article by Greenham and Friend [9] may be consulted. The interest in polyacetylene can be traced back at least to the report of high conductivity in charge transfer complexes formed with this polymer [10]. The fact that these polymers had simple structures, plus
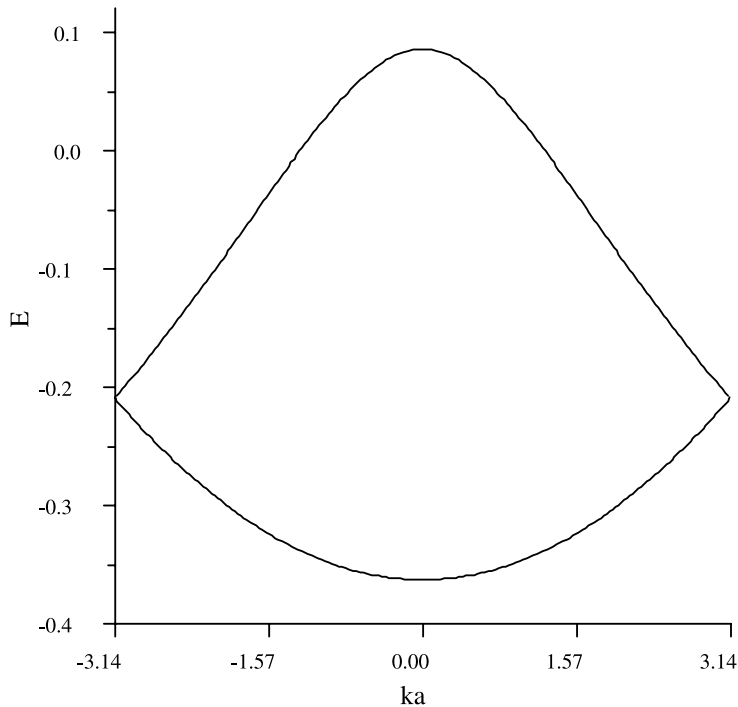

Figure 10.   Dispersion relation $E(\mathbf{k})$ in *trans*-polyacetylene without C–C bond alternation. Note the touching of the sub-bands and as a consequence the zero energy gap.
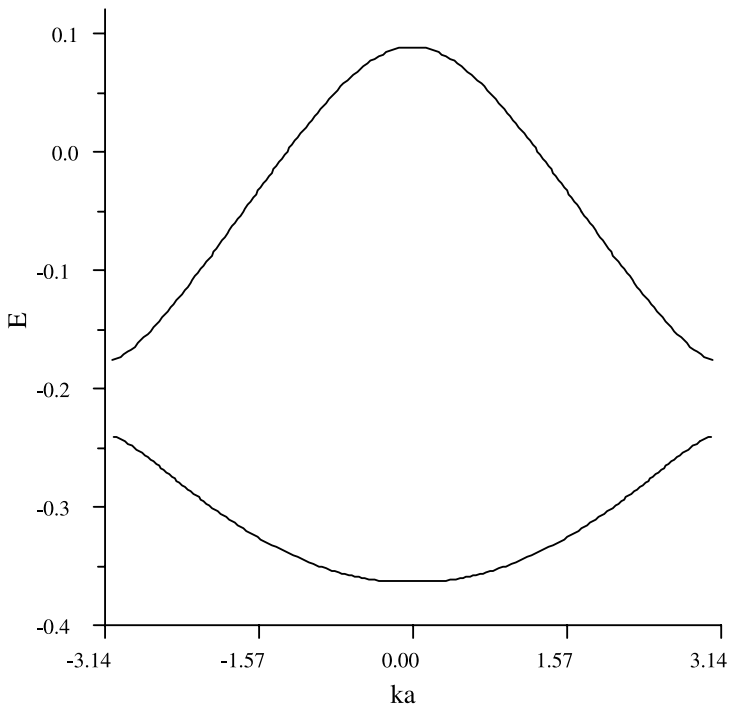
Figure 11. $E(\mathbf{k})$ for the *trans*-polyacetylene with alternating single and double C–C bonds of lengths $1.53\,\text{Å}$ and $1.35\,\text{Å}$, respectively.

the fact that they could be used as electrical conductors, was immediately attractive for device physics. Polyacetylene has proved to be the protypical conjugated polymer. It can exist in various isomeric forms and the trans-transoidal structure, usually termed simply *trans*-polyacetylene, known to be the thermodynamically stable isomer at room temperature, is depicted in figure 2(d).

Interest in the π-electronic structure of polyacetylene dates back at least to Lennard-Jones [11]. As the length of the conjugated chain is increased, the energy gap between the occupied π orbitals and the empty π^* orbitals reduces, though in the long chain limit the gap remains finite at a value of about $1.5\,\text{eV}$. The theoretical reasoning for this goes back at least to Longuet-Higgins and Salem [12]. We close this brief summary by commenting that the behaviour of the electrical conductivity with both acceptor and donor dopant is quite suggestive of conventional substitutional p and n doping of a semiconductor. Doping however is not now substitutional: the dopant species reside along the polymer and there is charge-transfer reaction that parallels the intercalation chemistry known for graphite (see [13]).

5. Formalism of the quantum network model (QNM)

We define a Schrödinger equation on a graph, a collection of edges (wires, links, lines, etc.) joined in vertices (nodes). Adopting the atomic units, on a link between two nodes i and j we have

$$\left[-\frac{1}{2} \frac{\partial^2}{\partial \lambda^2} + v_{ij}(\lambda) \right] \varphi_{ij}(\lambda) = \epsilon \varphi_{ij}(\lambda) \tag{14}$$

for an electron moving on such a graph [1,3]. equation (14) is a linear second-order homogeneous differential equation and has the general solution

$$\varphi_{ij}(\lambda) = F_{ij}(\lambda)\varphi_{ij}(0) + G_{ij}(\lambda)\varphi'_{ij}(0), \tag{15}$$

where F_{ij} satisfies (14) with initial conditions $F_{ij}(0) = 1$ and $F'_{ij}(0) = 0$, and G_{ij} satisfies (14) with initial conditions $G_{ij}(0) = 0$ and $G'_{ij}(0) = 1$. λ varies between 0 and l_{ij}, l_{ij} being the length of the link connecting the nodes (junctions) i and j. The boundary conditions on $\varphi_{ij}(0)$ and $\varphi'_{ij}(0)$ must be set according to the requirement that the Hamiltonian operator defined over the graph is self adjoint.

For two solutions η_{ij} and φ_{ij} of equation (14), this condition implies

$$\sum_{ij \text{ links}} \left[\eta^*_{ij} \frac{\partial \varphi_{ij}}{\partial \lambda} - \frac{\partial \eta^*_{ij}}{\partial \lambda} \varphi_{ij} \right]_0^{l_{ij}} = 0, \tag{16}$$

which is guaranteed by the more general relation [14]

$$\sum_{j=1}^{c_i} A_{kj} \varphi_{ij}(0) + \sum_{j=1}^{c_i} B_{kj} \varphi'_{ij}(0) = 0, \tag{17}$$

where c_i is the coordination number of the node i and **A** and **B** are $c_i \times c_i$ matrices chosen in such a way that $\mathbf{AB}^\dagger = \mathbf{BA}^\dagger$. Equation (17) in a more general sense takes the meaning of a Kirchoff's law at node i of the network. Thinking of realistic electron systems, from molecules to lattices, it is immediate to fix the continuity of the wave function at the vertices: this means

$$\varphi_{i1}(0) = \varphi_{i2}(0) = \cdots = \varphi_{ic_i}(0) = \Phi_i,$$
$$A_{kk} = 1, \quad A_{kk+1} = -1, \quad A_{kj} = 0, \quad (j \neq k, k+1), \tag{18}$$
$$B_{kj} = 0, \quad 1 \leqslant k \leqslant c_i - 1,$$

which leaves the following freedom

$$\begin{aligned} \sum_{j=1}^{c_i} \varphi'_{ij}(0) &= \zeta_i \Phi_i, \\ A_{c_i j} = \zeta_i, \qquad B_{c_i j} &= -1. \end{aligned} \tag{19}$$

Equation (19) have some resemblance with Kato's cusp condition which for example in the H atom ground state reads

$$\left(\frac{\partial \rho(r)}{\partial r}\right)_0 = -\frac{2}{a_0}\rho(0), \tag{20}$$

where $\rho(r)$ is the electron density: being the square of the ground-state wave function. Thus we expect that, if a vertex coincides with the position of a nucleus, ζ_i could be $\neq 0$ while is zero in other cases. For π-electron networks the nodes are located outside nuclei, owing to the nodal structure of the one-electron wave functions, the Ruedenberg and Scherr [1] condition is then validated by the above consideration. A full discussion on the relation between $\sum_j \varphi'_{ij}(0) = 0$ and the principle of current conservation is given in the Ruedenberg and Scherr [1] paper.

Instead, when nodes and wires are not coincident with atoms and bonds, **A** and **B**, according to (17), could have, in principle, very different matrix elements than in (18) and (19). Although, it has not yet been found in a realistic system of this type, the role of the two matrices, **A** and **B**, seems important in thinking about circuits for quantum computing [15].

In this respect, it is important to notice that when some of the nodes of the network are taken to infinity, the corresponding links become open channels, and in this case we can define a scattering matrix to relate incoming and scattered plane waves (the asymptotic free-particle wave functions along the open channels). For instance, if j is a node of the graph connected to infinity, we have (see, for example [16])

$$\psi_j^k(x) = \begin{cases} S_{jk}(q)\exp(iqx) \\ \exp(\text{-}iqx) + S_{kk}(q)\exp(iqx) & (j = k), \end{cases} \tag{21}$$

where all the nodes of the same type of j are labelled by k and where x varies along the line connecting k to infinity with origin at the node. **S** is the unitary scattering matrix. The notation in (21) establishes the direction of transmission. In the study of quantum networks, one of the most attractive aims is the construction of graphs which can realistically model physical systems, and determine a scattering matrix, for a given choice of open channels, which corresponds to one of the basic logical gates.

Turning back to a closed graph, it is possible to derive a set of equations which involves the wavefunction evaluated at all node positions. We combine equations (15), (18) and (19). From (15) we have at node j

$$\Phi_j = \varphi_{ij}(l_{ij}) = F_{ij}(l_{ij})\Phi_i + G_{ij}(l_{ij})\varphi'_{ij}(0) \tag{22}$$

and then from (19)

$$\sum_{j=1}^{c_i} \varphi'_{ij}(0) = \zeta_i \Phi_i = -\Phi_i \sum_{j=1}^{c_i} \frac{F_{ij}}{G_{ij}} + \sum_{j=1}^{c_i} \frac{\Phi_j}{G_{ij}}, \tag{23}$$

which defines a system of N equations, one at each vertex, and involving only the wave function evaluated at the nodes. Equation (23) has been studied in model lattices with one component in the unit cell, by putting $\zeta_i = 0$, $F_{ij} = F$ and $G_{ij} = G$ and evaluating F by solving the Schrödinger equation (14) for a model potential [4,17]. In this situation we have

$$c_i F \Phi_i = \sum_{j=1}^{c_i} \Phi_j . \tag{24}$$

In the more general case all possible F_{ij} and G_{ij} must be calculated by solving (14) along wires. It is interesting to look at the corresponding integral equations

$$F_{ij}(l_{ij}) = \cos q l_{ij} + 2 \int_0^{l_{ij}} \frac{\sin\left[q(l_{ij} - t)\right]}{q} v_{ij}(t) F_{ij}(t) \mathrm{d}t, \tag{25}$$

and

$$G_{ij}(l_{ij}) = \frac{\sin q l_{ij}}{q} + 2 \int_0^{l_{ij}} \frac{\sin\left[q(l_{ij} - t)\right]}{q} v_{ij}(t) G_{ij}(t) \mathrm{d}t, \tag{26}$$

where $q = \sqrt{2\epsilon}$. Through these equations one can attempt a perturbative solution in cases in which free-electrons are weakly perturbed by a potential v_{ij} along wires. It is also important to remark that $F_{ij}(l_{ij}) = F_{ji}(l_{ij})$ only if the potential is symmetrical along the link $i - j$, the same holds for G_{ij}. F and G are also connected by the constancy of the Wronskian

$$W = F(\lambda)G'(\lambda) - F'(\lambda)G(\lambda) = F(0)G'(0) - F'(0)G(0) = 1 . \tag{27}$$

In order to establish a bridge between the quantum network model here discussed and real electron systems, knowledge of both F and G functions is essential input. In the case of models satisfying equation (24) the unique value of F is given by connectivity [4,18]. Defining the connectivity matrix by the elements $H_{ij} = 1$ for linked i and j and $H_{ij} = 0$ otherwise, we can rearrange equation (24) to obtain the secular equation

$$\mathbf{Mf} = F\mathbf{f}, \tag{28}$$

where

$$M_{ij} = \frac{H_{ij}}{\sqrt{c_i c_j}}, \qquad f_i = \sqrt{c_i} \Phi_i \tag{29}$$

and in which the "so-called" form factor F is the eigenvalue of the transformed connectivity matrix **M**. In the case of an infinite periodic system equation (28) is diagonalized by applying Bloch's theorem to Φ_i.

In different cases we must apply equation (23) without approximations. Let us take for example the π orbitals of a butadiene molecule (see figure 2(c)). In this case we can put $\zeta_i = 0$ and from (23) we get the system of equations

$$F_s \Phi_1 = \Phi_2,$$
$$\left(\frac{F_s}{G_s} + \frac{F_l}{G_l} \right) \Phi_2 = \frac{1}{G_s} \Phi_1 + \frac{1}{G_l} \Phi_3,$$
$$\left(\frac{F_s}{G_s} + \frac{F_l}{G_l} \right) \Phi_3 = \frac{1}{G_l} \Phi_2 + \frac{1}{G_s} \Phi_4,$$
$$F_s \Phi_4 = \Phi_3$$

(30)

in which the subscript s indicates the short bonds (between carbons 1 and 2 and between carbons 3 and 4) and l the long bond (between carbons 2 and 3). F derived from (28) is always in the interval [–1,1] (allowed values), while in the more general case as in (30) could be also >1 or <-1. The solution of (30) requires the knowledge of both the F and G functions and consequently of the potential along wires. Such a potential is normally unknown and in the development of the quantum network model for applications to real systems its derivation is a crucial point. Inside wires the potential behaves as a barrier because the overall potential shows clearly minima at the nuclear positions. For a symmetric v_{ij} potential one can resort to a reliable approximation like

$$v_{ij}(\lambda) = v_{ij}(0) + \Delta_{ij} \sin^2 \left(\frac{\pi \lambda}{l_{ij}} \right),$$

(31)

where the constants $v_{ij}(0)$ and Δ_{ij} may be determined, for example, by fitting ab initio data obtained for a small molecule. As in a self consistent field approach, both $v_{ij}(0)$ and Δ_{ij} could, in principle, be dependent on the energy eigenvalue ϵ of the Schrödinger equation (14).

By way of example, in figure 12 the computed *ab initio* molecular electrostatic potential is plotted along a broken line parallel to the carbon chain and 0.5 Å above, more or less inside the upper lobe of the π orbitals, calculated for neutral and ionized butadiene. It is evident, from this Figure, that the barrier is higher for the long C–C bond and that approximately the barrier height is not very sensitive to the filling of π orbitals while instead the curves are shifted in the three cases.

A further difficult aspect in connecting the model to real systems is the confinement of wires in perpendicular directions. In the present model we assume an infinitely small thickness, while normally we have not this situation. Some discussion on "fattened graphs" is given in [19].

6.   Summary and future directions

Following specific examples of graphene and then boron nitride layers, Section 5 sets out a rather general compact formulation of the QNM. The model, as we have demonstrated is sufficiently simple that energy-wave vector ($E(\mathbf{k})$) relations and the associated density of states can readily be obtained on a personal computer.

In addition to the graphene sheet in Section 2, C nanotubes [20, 21] can be treated by "wrapping" the graphene sheet in various ways (see figure 13). The QNM has been applied to the electronic structure of B nanotubes for various wrappings in [18].

Also of interest is the possible generalization of the band gap calculation presented for *trans*-polyacetylene in Section 4 to a wide class of potentially interesting polymers for device physics. Among these are numbered polydiacetylene, with a π sub-band gap near 1.7 eV [9], *para*-polyphenyl (PPP) 3 eV and polypyrrole (PPY) with a gap of 3.1 eV. In PPP, the enhanced energy separation between the π sub-bands arises from (a) the introduction of benzene rings and (b) the
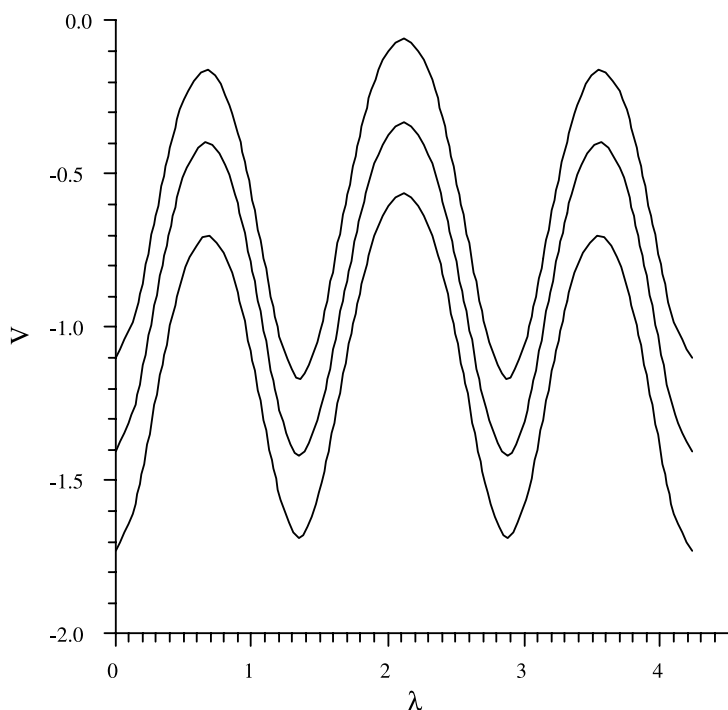

Figure 12.   Molecular electrostatic potential along a broken line 0.5 Å above the C_1–C_2–C_3–C_4 chain for $C_4H_6^+$ (lower curve), C_4H_6 and $C_4H_6^-$ (upper curve). Energies are in hartree and length in Å.
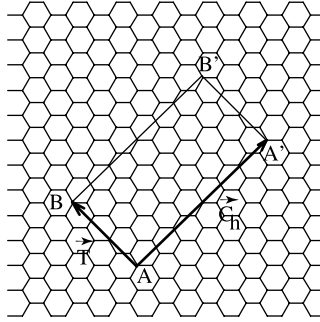
Figure 13.   Shows a particular wrapping of a graphene layer into a C nanotube related to the type discovered by Iijima [20]. Points A and A′, as points B and B′, are brougth to coincidence. The part enclosed in the wrapped rectangle forms the unit cell of the nanotube. $\vec{T}$ and $\vec{C}_h$ are the translational and the chiral vectors, respectively (see the book by Saito et al. [21] for a full discussion).

consequential effect of the departure of these from planarity. It is a question of interest for the future as to whether the QNM can be adapted to deal with this situation with more modest effort than full electronic band structure calculations.

Doping has been referred to in Section 4 and an application of the QNM to treat various type of atomic defects in an otherwise perfect network has been set out by Mills and Montroll [17].

Finally, and more ambitiously, disorder can be introduced into the QNM, as treated initially by Dancz et al. [22], and later, and much more mathematically by Ringwood [23]. In this study, the simplest form of the QNM presented here, namely the free-electron network model (with $V = 0$ along all wires) is reformulated in terms of restricted random walks. Ringwood's work is suitable for the study of topologically disordered networks [24, 25]. Whereas in the earlier study of Dancz et al., the network model is used to study localization in disordered systems, and due to the absence of Bloch's theorem, since **k** the wave vector can no longer be used to characterise the energy states, statistical arguments are invoked and a Boltzmann equation for the system is derived, Ringwood calculates the Feynman propagator within his restricted random walk framework. One consequence for the density of states of the graphene layer (see figure 6) is that the spikiness (arising from the so-called Van Hove singularities [26]) is smeared out by disorder. Also interesting questions arise as to whether the delocalized Bloch wave functions appropriate to perfect crystals become localised by sufficient disorder in the QNM.

References

[1] K. Ruedenberg and C.W. Scherr, J. Chem. Phys. 21 (1953) 1565.
[2] C.A. Coulson, Proc. Phys. Soc. (Lond.) A 67 (1954) 608.
[3] C.A. Coulson, Proc. Phys. Soc. (Lond.) A 68 (1955) 1129.

 [4] E.W. Montroll, J. Math. Phys. 11 (1970) 635.
 [5] L. Pauling, J. Chem. Phys. 4 (1936) 673.
 [6] H. Kuhn, J. Chem. Phys. 16 (1948) 840.
 [7] J.R. Platt, J. Chem. Phys. 17 (1949) 484.
 [8] R. McWeeny, *Quantum Mechanics: Methods and Basic Applications* (Pergamon Press, Oxford, 1973).
 [9] N.C. Greenham and R.H. Friend, Solid State Phys. 49 (1995) 1.
[10] C.K. Chiang, C.R. Fincher Jr., Y.W. Park, A.J. Heeger, H. Shirakawa, E.J. Louis, S.C. Gau and A.G. MacDiarmid, Phys. Rev. Lett. 39 (1977) 1098.
[11] J.E. Lennard-Jones, Proc. R. Soc. Lond. A 158 (1937) 280.
[12] H.C. Longuet-Higgins and L. Salem, Proc. R. Soc. Lond. A 251 (1959) 172.
[13] M.S. Dresselhaus and G. Dresselhaus, Adv. Phys. 30 (1981) 139.
[14] V. Kostrykin and R. Schrader, J. Phys. A: Math. Gen. 32 (1999) 595.
[15] V. Kostrykin and R. Schrader, Fortschr. Phys. 48 (2000) 703.
[16] P. Kurasov and F. Stenberg, J. Phys. A: Math. Gen. 35 (2002) 101.
[17] R.G.J. Mills and E.W. Montroll, J. Math. Phys. 11 (1970) 2525.
[18] F.E. Leys, C. Amovilli and N.H. March, J. Chem. Inf. Comput. Sci. 44 (2004) 122. (released on the web)
[19] P. Kuchment, Wave Random Media 12 (2002) R1.
[20] S. Iijima, Nature 354 (1991) 56.
[21] R. Saito, G. Dresselhaus and M.S. Dresselhaus, *Physical Properties of Carbon Nanotubes* (Imperial College Press, London, 1998).
[22] J. Dancz, S.F. Edwards and N.H. March, J. Phys. C 6 (1973) 873.
[23] G.A. Ringwood, J. Math. Phys. 22 (1981) 96.
[24] P.G. Doyle and J.L. Snell, *Random Walks and Electric Networks* (Mathematical Association of America, Washington DC, 1984).
[25] A.H. Zemanian, IEEE Trans. Circuits Syst. 35 (1988) 1346.
[26] J.M. Ziman, *Principles of the Theory of Solids* (University Press, Cambridge, 1979).